AIP | Applied Physics Letters

High Mg-content wurtzite MgZnO alloys and their application in deep-ultraviolet light-emitters pumped by accelerated electrons

Pei-Nan Ni, Chong-Xin Shan, Bing-Hui Li, and De-Zhen Shen

Citation: Applied Physics Letters **104**, 032107 (2014); doi: 10.1063/1.4862789
View online: http://dx.doi.org/10.1063/1.4862789
View Table of Contents: http://scitation.aip.org/content/aip/journal/apl/104/3?ver=pdfcov
Published by the AIP Publishing

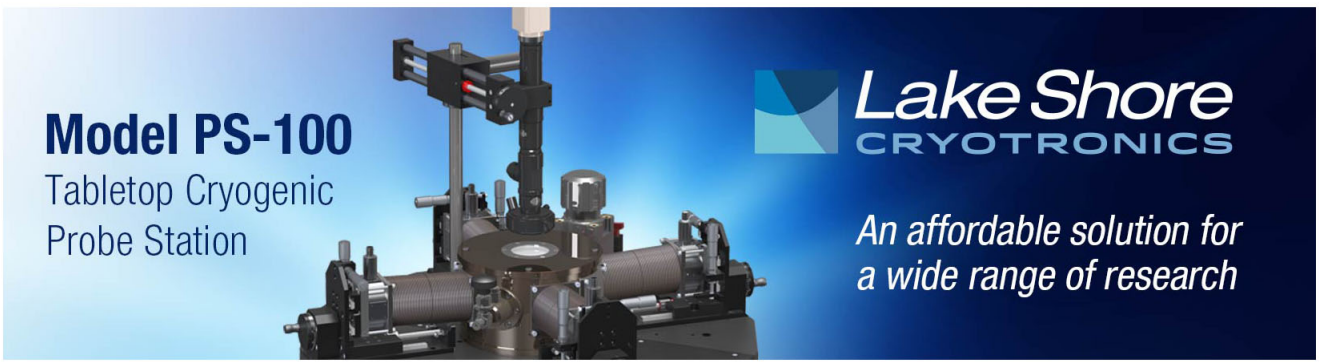

High Mg-content wurtzite MgZnO alloys and their application in deep-ultraviolet light-emitters pumped by accelerated electrons

Pei-Nan Ni,[1,2] Chong-Xin Shan,[1,a)] Bing-Hui Li,[1] and De-Zhen Shen[1,a)]
[1]*State Key Laboratory of Luminescence and Applications, Changchun Institute of Optics, Fine Mechanics and Physics, Chinese Academy of Sciences, Changchun 130033, China*
[2]*University of Chinese Academy of Sciences, Beijing 100049, China*

(Received 23 October 2013; accepted 5 January 2014; published online 24 January 2014)

High Mg-content single-phase wurtzite MgZnO alloys with a bandgap of 4.35 eV have been obtained on sapphire substrate by introducing a composition-gradient $Mg_xZn_{1-x}O$ buffer layer. By employing the accelerated electrons obtained in a solid-state structure as an excitation source, an emission at around 285 nm, which is originated from the near-band-edge emission of the $Mg_{0.51}Zn_{0.49}O$ active layer, has been observed. The results reported in this paper may provide a promising route to high performance deep-ultraviolet light-emitting devices by bypassing the challenging doping issues of wide bandgap semiconductors. © *2014 AIP Publishing LLC*. [http://dx.doi.org/10.1063/1.4862789]

Deep-ultraviolet (DUV) light-emitters (with operation wavelength shorter than 300 nm) have a wide range of potential applications in high-density data storage, water and air purification, detection of chemical/biological agents, medical diagnosis, etc.[1–3] Nevertheless, currently the most frequently used DUV light source (i.e., mercury lamp) is usually bulky and costly currently, even worse, it brings the risk of the possible heavy metal pollution, all of which hinder the practical use of such DUV light source in many areas. As a promising alternative to mercury lamp, wide bandgap semiconductor based DUV light source has a variety of figure-of-merits such as low-power consumption, high-efficiency, compact size, long lifetime, low pollution, etc., thus much attention has been paid to this area in recent years.[4–7] Conventionally, efficient semiconductor based light sources are realized in *pn* junctions. However, although some reports have demonstrated DUV emissions from wide bandgap semiconductor based *pn* junctions,[8–10] with the bandgap increases, both the *p*-type doping and *n*-type doping of wide bandgap semiconductors turn out to be a huge challenge due to the relatively large activation energy of acceptors and donors,[6,11–13] which makes *pn* junction structure for semiconductor based DUV emissions problematic. It has been demonstrated recently that wide bandgap semiconductor based DUV emissions can be realized by employing electron beam as the excitation source.[14–16] Nevertheless, the electron beam in these devices is usually generated in vacuum under high voltage conditions, making these devices bulky and impairing their usefulness.

MgZnO, with a tunable bandgap from 3.37 eV to 7.8 eV, which covers a broad portion of the DUV spectrum range, is a promising candidate for the DUV optoelectronic devices.[17,18] Moreover, compared with other wide bandgap semiconductors, its unique features, such as the high resistance to radiation, the amenability to conventional wet chemistry etching, the environmentally friendly characters, and the relatively low growth temperatures, make MgZnO alloys promising candidate as the DUV light-emitters under the excitation of accelerated electrons.[19–22] Nevertheless, since MgO prefers to crystallize in cubic rock-salt structure, while ZnO in hexagonal wurtzite structure, it is difficult to obtain a single-phase wurtzite MgZnO (W-MgZnO) with high Mg content, especially when extending its bandgap into the DUV region, due to the well-known phase-segregation problems.[23–25] Although great efforts have been devoted to the synthesis of high Mg-content W-MgZnO alloys, such as the use of a high-quality ZnO buffer layer,[24] employing a quasi-homo MgZnO buffer with a low-Mg content,[25] no report on DUV emissions from single-phase W-MgZnO can be found up to now. This is largely limited by the relatively low optical quality which is suffering from the strain that arises from the mismatch in both thermal expansion coefficients and lattice constants between the cladding layer and the buffer layer or the substrate. A composition-gradient buffer layer (CGBL) has been demonstrated to effectively offset tensile growth stresses in AlGaN/GaN, AlGaAs/GaAs, and SiGe/Si heterostructures, which can bring about gradual strain-relaxation with misfit dislocations being distributed throughout the buffer layer instead of being concentrated at the interface.[26–28] Therefore, the CGBL may help to obtain high Mg-content single-phase W-MgZnO alloys with high crystallization quality.

In this Letter, single-phase W-MgZnO alloys with a bandgap of 4.35 eV have been obtained on sapphire substrate by introducing a $Mg_xZn_{1-x}O$ CGBL via molecular-beam epitaxy (MBE) technique. DUV light-emitting devices have been designed and fabricated from Au/MgO/W-$Mg_{0.51}Zn_{0.49}O$/$Mg_xZn_{1-x}O$/*n*-ZnO structure. With a negative voltage applied onto the Au electrode, electrons from the Au electrode will enter into the MgO layer and be accelerated greatly due to the relatively large electric field in this layer. These accelerated electrons will excite the W-$Mg_{0.51}Zn_{0.49}O$ layer once they gain enough energy. In this way, DUV emissions at around 285 nm, which come from the near-band-edge (NBE) emission of the W-$Mg_{0.51}Zn_{0.49}O$ active layer, have been observed.

The MgZnO alloys were grown on *c*-plane sapphire substrates in a VG V80H plasma-assisted MBE technique. The precursors used for the growth were elemental zinc (6N in purity), elemental magnesium (6N in purity), and O_2 gas (5N in

a)Authors to whom correspondence should be addressed. Electronic addresses: shancx@ciomp.ac.cn and shendz@ciomp.ac.cn

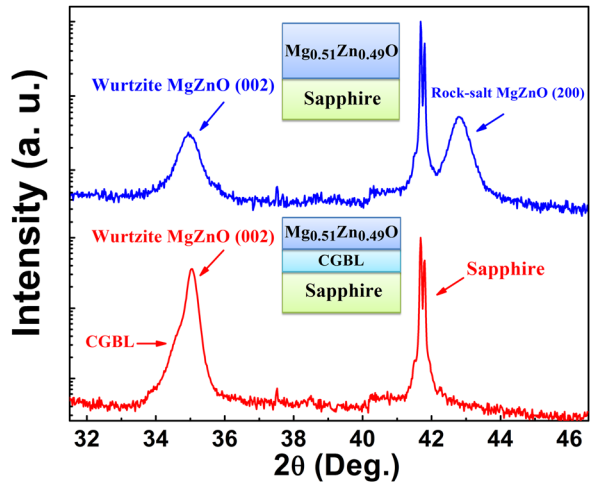

FIG. 1. X-ray diffraction pattern of the $Mg_{0.51}Zn_{0.49}O$ films with and without the $Mg_xZn_{1-x}O$ CGBL, and the insets show the diagram of each structure.

purity). The O_2 gas was activated in an Oxford Applied Research plasma cell (Model HD25) with radio frequency operating at 13.56 MHz at a fixed power of 300 W. During the growth process, the substrate temperature was fixed at 500 °C and the chamber pressure at 2.5×10^{-5} mbar. Before the deposition of the $Mg_{0.51}Zn_{0.49}O$ layer, a $Mg_xZn_{1-x}O$ CGBL with x changing gradually from 0 to 0.51 was first deposited onto the substrate. To form the Au/MgO/$Mg_{0.51}Zn_{0.49}O$/$Mg_xZn_{1-x}O$/*n*-ZnO structure, a 550 nm ZnO layer with an electron concentration of 3.2×10^{18} cm^{-3} and a Hall mobility of 65 cm^2 V^{-1} s^{-1} was employed as the conductive layer. Then a 320 nm $Mg_xZn_{1-x}O$ CGBL and a 310 nm $Mg_{0.51}Zn_{0.49}O$ active layer was deposited onto the ZnO conductive layer in sequence. After that, a 100 nm MgO layer was deposited onto the $Mg_{0.51}Zn_{0.49}O$ layer in a reactive radio-frequency magnetron sputtering technique using a 99.99% magnesium target at a radio frequency power of 190 W. Finally, a semitransparent thin Au layer was deposited onto the MgO layer and an In layer onto the ZnO layer in vacuum evaporation to act as electrodes.

The electrical properties of the films were characterized in a Hall measurement system (LakeShore 7707). A Bruker-D8 Discover X-ray diffractometer (XRD) with Cu-Kα radiation (1.54 Å) was used to evaluate the crystalline properties of the layers. The Mg content in the MgZnO layer was determined by energy-dispersive X-ray spectroscopy. The optical absorption spectra of the layers were recorded in a Shimadzu UV-3101PC spectrophotometer. Photoluminescence (PL) spectra of the layers were measured in an Omni-λ5008 spectrometer equipped with Andor iDus CCD, employing a He-Ag laser ($\lambda = 224$ nm) as the excitation source. The current-voltage (I–V) characteristics of the structure were measured using a Keithley 2611A SourceMeter, and the emission spectra were recorded in a Hitachi F4500 spectrometer with a continuous-current power source at room temperature.

Figure 1 shows the XRD θ-2θ pattern of the $Mg_{0.51}Zn_{0.49}O$ alloys deposited on sapphire substrate with or without a $Mg_xZn_{1-x}O$ CGBL. For the samples with the $Mg_xZn_{1-x}O$ CGBL, besides the diffraction peak from the sapphire (006) facet, only a peak at around 35.0° is visible in the pattern, which can be attributed to the diffraction from wurtzite structured MgZnO (002) plane. Note that this peak shows a significant shift to large-angle side compared with that from ZnO (002) which is typically detected at 34.4°, indicating the incorporation of Mg into ZnO.[29] Meanwhile, this peak shows a slight asymmetry with a weak shoulder in the small-angle side, which may come from the $Mg_xZn_{1-x}O$ CGBL. Meanwhile, no other signal can be found, revealing that phase-separation that is frequently observed in MgZnO alloys with high Mg-content is absent in our structure. In contrast, the XRD θ-2θ pattern of the $Mg_{0.51}Zn_{0.49}O$ layer that deposited directly on the sapphire substrate without the $Mg_xZn_{1-x}O$ CGBL shows two peaks at 35.0° and 42.8°, which correspond to the wurtzite MgZnO (002) plane and the rock-salt MgZnO (200) plane, suggesting the occurrence of phase-separation in the $Mg_{0.51}Zn_{0.49}O$ layer. Furthermore, as can be seen, the intensity of the peak at 35.0° for the $Mg_{0.51}Zn_{0.49}O$ layer without the $Mg_xZn_{1-x}O$ CGBL is much smaller than that with the CGBL layer. The above results prove that the $Mg_xZn_{1-x}O$ CGBL is essential to fix strictly the crystal structure of MgZnO layer deposited onto it to wurtzite against the tendency of phase separation as well as to improve its crystallization quality.

Room temperature PL spectrum of the $Mg_{0.51}Zn_{0.49}O$ alloys with the $Mg_xZn_{1-x}O$ CGBL is illustrated in Fig. 2(a). An emission at about 283 nm dominates the spectrum, which can be attributed to the NBE emission of the $Mg_{0.51}Zn_{0.49}O$ layer. Meanwhile, a broad shoulder can be found in the range of 300–330 nm, which is proved to come from the $Mg_xZn_{1-x}O$ CGBL by comparing it with the PL spectrum of the $Mg_xZn_{1-x}O$ CGBL without $Mg_{0.51}Zn_{0.49}O$ layer on top of it, (Not shown here). To determine the optical bandgap of the $Mg_{0.51}Zn_{0.49}O$ layer, the optical absorption spectrum of

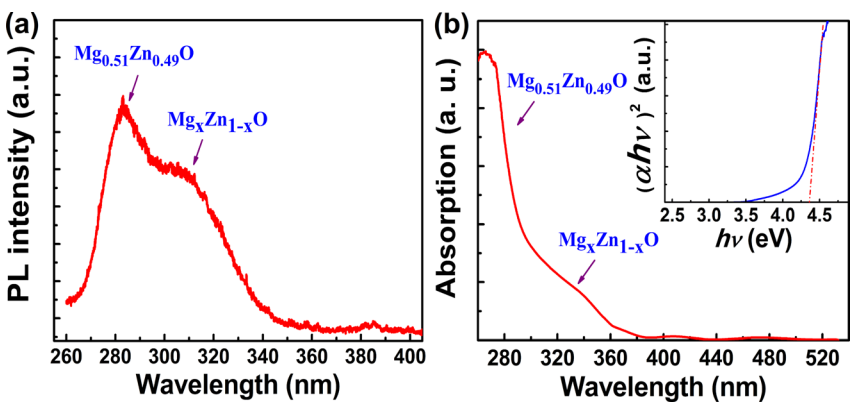

FIG. 2. PL spectrum (a) and absorption spectrum (b) of the W-$Mg_{0.51}Zn_{0.49}O$ film grown on sapphire substrate with $Mg_xZn_{1-x}O$ CGBL, and the inset of (b) shows a plot of $(ahv)^2$ *vs* hv for the sample.

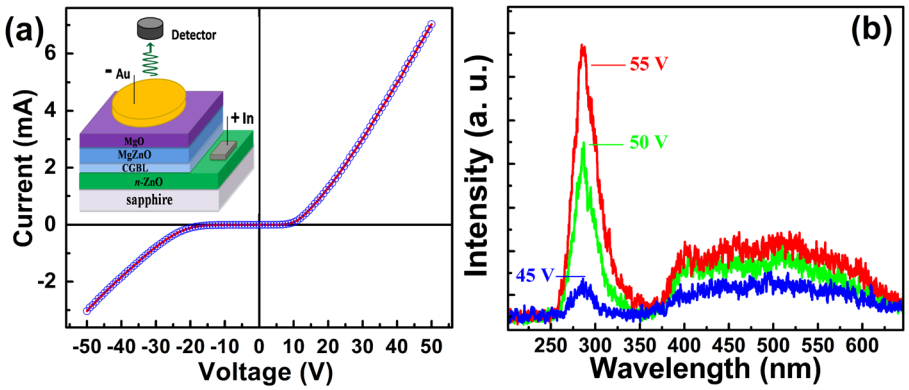

FIG. 3. (a) Current-voltage characteristics of the Au/MgO/$Mg_{0.51}Zn_{0.49}O$/$Mg_xZn_{1-x}O$/*n*-ZnO structure, and the inset shows the schematic diagram and emission recording geometry of the structure. (b) Emission spectra of the structure under different reverse bias voltages.

the MgZnO alloys with the $Mg_xZn_{1-x}O$ CGBL is measured and shown in Fig. 2(b). Two absorption components coming from the $Mg_{0.51}Zn_{0.49}O$ layer and the $Mg_xZn_{1-x}O$ CGBL, indicated by the arrows, can be observed clearly. The bandgap of the $Mg_{0.51}Zn_{0.49}O$ layer is fitted to be 4.35 eV from the plot of $(ahv)^2$ *vs* hv (a and hv are the absorption coefficient and photon energy, respectively), as shown in the inset of Fig. 2(b). The bandgap deduced from the absorption spectrum is in reasonable agreement with the PL peak at 283 nm (corresponding to an energy value of 4.38 eV) of the $Mg_{0.51}Zn_{0.49}O$ layer shown in Fig. 2(a).

Based on the obtained single-phase W-$Mg_{0.51}Zn_{0.49}O$ layer, DUV light-emitting devices have been fabricated from Au/MgO/W-$Mg_{0.51}Zn_{0.49}O$/$Mg_xZn_{1-x}O$/*n*-ZnO structure. The inset of Fig. 3(a) shows the schematic diagram and emission recording geometry of this structure. The *I-V* characteristics of the structure are shown in Fig. 3(a), where the reverse bias is defined as the situation that a negative voltage is applied onto the Au contact. The *I-V* curve shows an asymmetric shape with an obvious rectifying behavior. The characteristic emission spectra of the structure under different reverse bias are shown in Fig. 3(b). Under a reverse bias of 45 V, an obvious emission at around 285 nm can be observed. Considering that the wavelength of the peak (285 nm) is almost identical to that of the PL of the $Mg_{0.51}Zn_{0.49}O$ layer (283 nm), it can be attributed to the NBE emission of this layer. Moreover, as evidenced from the figure, the emissions from the $Mg_{0.51}Zn_{0.49}O$ layer increase significantly with further increasing the bias, while a weak defect-related emission appears in the visible region and changes little with the bias. The obvious DUV emissions from this structure indicate the promising application of the MgZnO alloys as DUV light-emitters. Note that the DUV emissions have been realized by bypassing the troublesome issues of both *p*-type doping and *n*-type doping of wide bandgap semiconductors, which are known to be more challenging as the bandgap increases.[30–32] Therefore, it may provide a route to wide bandgap semiconductor based high performance DUV light-emitting devices.

The mechanism for the above emissions observed from the Au/MgO/W-$Mg_{0.51}Zn_{0.49}O$/$Mg_xZn_{1-x}O$/*n*-ZnO structure can be understood in terms of the band alignment of the structure, as shown in Fig. 4. Under reverse bias, such as at 45 V, most of the voltage would be applied onto the MgO layer due to its dielectric nature. As a result, both the conduction and valence bands of the MgO layer will bend drastically, and the voltage drop across the MgO (V_{ox}) will be much larger than the barrier height for the electrons at the Au side ($\Phi_{ox} = 4.3$ eV). Under this condition, the effective width of the triangular barrier that hinders the tunneling of the electrons from the Au electrode to the MgO layer will be reduced significantly, thus many electrons can tunnel directly into the conduction band of the MgO layer through the Fowler-Nordheim (FN) tunneling process.[33] Considering that the thickness of the MgO layer is only about 100 nm, the electric field in the MgO will be very high (e.g., as high as 4.5×10^6 Vcm^{-1} at 45 V). Thus, when the electrons coming from the Au electrode enter into this layer, they will be accelerated greatly by such a high field and gain much kinetic energy. Once these accelerated electrons enter into the $Mg_{0.51}Zn_{0.49}O$ active layer, they will release their energy by exciting the electrons in the valence band of this layer into its conduction band, giving rise to free electrons and holes.[34] Then, the electrons in the conduction band may recombine radiatively with the holes in the valence band to give DUV emissions. Note that the electrons were accelerated in the

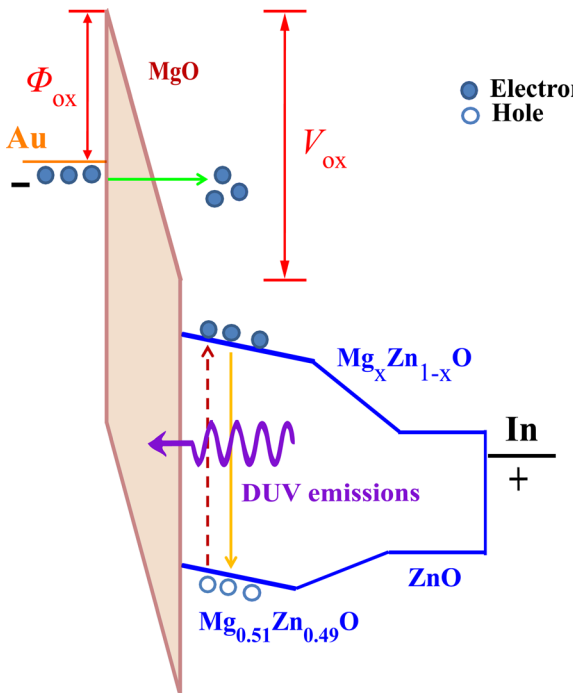

FIG. 4. Band diagram of the Au/MgO/$Mg_{0.51}Zn_{0.49}O$/$Mg_xZn_{1-x}O$/*n*-ZnO structure under reverse bias.

MgO layer in this structure rather than in vacuum condition as most other situations,[14–16,35] which helps to realize DUV emissions in small sized devices. Note that the whole thickness of this structure is estimated to be hundreds of nanometers. Since small size and portability are preferred for practical use in many cases, such a compact and simple structure may find potential applications in some fields that is strictly required in size or space.[16,36] It is also worth noting that UV emissions have been previously reported from the metal-insulator-semiconductor (MIS) structure under forward bias based on the impact ionization process taking place in the insulator layer.[17,37] Since the threshold energy for a phononless ionization process initiated by an electron can be expressed by the following formula:[38]

$$E_{th} = E_g\left(\frac{2+\gamma}{1+\gamma}\right), \quad (1)$$

where E_g is the bandgap energy and γ is the ratio between the effective masses of the electrons in the conduction and valence bands, one can see that the threshold energy increases with E_g. Therefore, it means that the emission mechanism under the excitation of accelerated electrons requires a much lower working bias voltage than that of the MIS structure at forward bias.

In conclusion, single-phase wurtzite $Mg_{0.51}Zn_{0.49}O$ alloys with a bandgap of 4.35 eV have been obtained on sapphire substrate via MBE technique by introducing a $Mg_xZn_{1-x}O$ CGBL, which is found favorable to prevent phase-separation in the MgZnO layer. DUV emissions have been realized from the $Mg_{0.51}Zn_{0.49}O$ alloys by designing a Au/MgO/$Mg_{0.51}Zn_{0.49}O$/$Mg_xZn_{1-x}O$/*n*-ZnO structure under the excitation of accelerated electrons. The results reported in this paper may provide a feasible method to obtain high Mg-content single-phase wurtzite MgZnO alloys with high crystallization quality and a promising alternative route to low-cost, small-sized DUV light sources by bypassing the challenging doping issues of wide bandgap semiconductors.

This work was supported by the National Basic Research Program of China (No. 2011CB302005), the Natural Science Foundation of China (Nos. 11074248, 11134009, 10974197, 11374296, and 61177040), and the Science and Technology Developing Project of Jilin Province (No. 20111801).

[1]T. M. Al Tahtamouni, N. Nepal, J. Y. Lin, H. X. Jiang, and W. W. Chow, Appl. Phys. Lett. **89**, 131922 (2006).
[2]Y. Kubota, K. Watanabe, O. Tsuda, and T. Taniguchi, Science **317**, 932 (2007).
[3]T. Kinoshita, T. Obata, H. Yanagi, and S. Inoue, Appl. Phys. Lett. **102**, 012105 (2013).
[4]V. Adivarahan, A. Heidari, B. Zhang, Q. Fareed, S. Hwang, M. Islam, and A. Khan, Appl. Phys. Express **2**, 102101 (2009).
[5]H. Hirayama, N. Noguchi, T. Yatabe, and N. Kamata, Appl. Phys. Express **1**, 051101, (2008).
[6]Y. Taniyasu, M. Kasu, and T. Makimoto, Nature **441**, 325 (2006).
[7]Y. Aoyagi and N. Kurose, Appl. Phys. Lett. **102**, 041114 (2013).
[8]S. Koizumi, K. Watanabe, M. Hasegawa, and H. Kanda, Science **292**, 1899 (2001).
[9]C. G. Moe, M. L. Reed, G. A. Garrett, A. V. Sampath, T. Alexander, H. Shen, M. Wraback, Y. Bilenko, M. Shatalov, J. W. Yang, W. H. Sun, J. Y. Deng, and R. Gaska, Appl. Phys. Lett. **96**, 213512 (2010).
[10]H. Hirayama, S. Fujikawa, N. Noguchi, J. Norimatsu, T. Takano, K. Tsubaki, and N. Kamata, Phys. Status Solidi A **206**, 1176 (2009).
[11]P. Bogusławski and J. Bernholc, Phys. Rev. B **56**, 9496 (1997).
[12]D. C. Look, B. Claflin, Ya. I. Alivov, and S. J. Park, Phys. Status Solidi A **201**, 2203 (2004).
[13]M. A. Thomas and J. B. Cui, J. Phys. Chem. Lett. **1**, 1090 (2010).
[14]T. Oto, R. G. Banal, K. Kataoka, M. Funato, and Y. Kawakami, Nature Photon. **4**, 767 (2010).
[15]K. Watanabe, T. Taniguchi, and H. Kanda, Nature Mater. **3**, 404 (2004).
[16]K. Watanabe, T. Taniguchi, T. Niiyama, K. Miya, and M. Taniguchi, Nature Photon. **3**, 591 (2009).
[17]H. Zhu, C. X. Shan, B. H. Li, Z. Z. Zhang, B. Yao, and D. Z. Shen, Appl. Phys. Lett. **99**, 101110 (2011).
[18]Y. N. Hou, Z. X. Mei, Z. L. Liu, T. C. Zhang, and X. L. Du, Appl. Phys. Lett. **98**, 103506 (2011).
[19]W. Yang, S. S. Hullavarad, B. Nagaraj, I. Takeuchi, R. P. Sharma, T. Venkatesan, R. D. Vispute, and H. Shen, Appl. Phys. Lett. **82**, 3424 (2003).
[20]Y. M. Zhao, J. Y. Zhang, D. Y. Jiang, C. X. Shan, Z. Z. Zhang, B. Yao, D. X. Zhao, and D. Z. Shen, ACS Appl. Mater. Interfaces **1**, 2428 (2009).
[21]N. B. Chen and C. H. Sui, Mater. Sci. Eng., B **126**, 16 (2006).
[22]V. Etacheri, R. Roshan, and V. Kumar, ACS Appl. Mater. Interfaces **4**, 2717 (2012).
[23]I. V. Maznichenko, A. Ernst, M. Bouhassoune, J. Henk, M. Däne, M. Lüders, P. Bruno, W. Hergert, I. Mertig, Z. Szotek, and W. M. Temmerman, Phys. Rev. B **80**, 144101 (2009).
[24]T. Takagi, H. Tanaka, S. Fujita, and S. Fujita, Jpn. J. Appl. Phys., Part 2 **42**, L401 (2003).
[25]Z. L. Liu, Z. X. Mei, T. C. Zhang, Y. P. Liu, Y. Guo, X. L. Du, A. Hallen, J. J. Zhu, and A. Yu. Kuznetsov, J. Cryst. Growth **311**, 4356 (2009).
[26]J. D. Acord, X. Weng, E. C. Dickey, D. W. Snyder, and J. M. Redwing, J. Cryst. Growth **310**, 2314 (2008).
[27]T. Hayakawa, T. Suyama, M. Kondo, K. Takahashi, S. Yamamoto, and T. Hijikata, Appl. Phys. Lett. **49**, 191 (1986).
[28]T. S. Yoon, J. Liu, A. M. Noori, M. S. Goorsky, and Y. H. Xie, Appl. Phys. Lett. **87**, 012104 (2005).
[29]A. Ohtomo, M. Kawasaki, T. Koida, K. Masubuchi, H. Koinuma, Y. Sakurai, Y. Yoshida, T. Yasuda, and Y. Segawa, Appl. Phys. Lett. **72**, 2466 (1998).
[30]J. Simon, V. Protasenko, C. Lian, H. Xing, and D. Jena, Science **327**, 60 (2010).
[31]A. Fujioka, T. Misaki, T. Murayama, Y. Narukawa, and T. Mukai, Appl. Phys. Express **3**, 041001 (2010).
[32]L. Zhang, K. Ding, J. C. Yan, J. X. Wang, Y. P. Zeng, T. B. Wei, Y. Y. Li, B. J. Sun, R. F. Duan, and J. M. Li, Appl. Phys. Lett. **97**, 062103 (2010).
[33]S. Singh, *Practical Quantum Mechanics* (Springer, 1974).
[34]P. N. Ni, C. X. Shan, S. P. Wang, B. H. Li, Z. Z. Zhang, and D. Z. Shen, Opt. Lett. **37**, 1568 (2012).
[35]M. D. Tiberi, V. I. Kozlovsky, and P. I. Kuznetsov, Phys. Status Solidi B **247**, 1547 (2010).
[36]Y. Shimahara, H. Miyake, K. Hiramatsu, F. Fukuyo, T. Okada, H. Takaoka, and H. Yoshida, Appl. Phys. Express **4**, 042103 (2011).
[37]P. L. Chen, X. Y. Ma, and D. R. Yang, Appl. Phys. Lett. **89**, 111112 (2006).
[38]C. L. Anderson and C. R. Crowell, Phys. Rev. B **5**, 2267 (1972).